

Two-dimensional and three-dimensional simulation of magnetic relaxation in frustrated spin-chain systems: $\text{Ca}_3\text{Co}_2\text{O}_6$

Yu. B. Kudasov,* A. S. Korshunov, V. N. Pavlov, and D. A. Maslov

Sarov Physics and Technology Institute, National Research Nuclear University "MEPhI", Dukhov street 6, Sarov, 607188, Russia

(Received 22 September 2010; revised manuscript received 24 January 2011; published 17 March 2011)

A response of a triangular spin-chain system to a step variation of an external magnetic field is investigated in the framework of the 2D and 3D Glauber dynamics. It is shown that an unusual relaxation process observed experimentally at intermediate magnetic fields in $\text{Ca}_3\text{Co}_2\text{O}_6$ is related to the growth of a domain size and the transition to a monodomain magnetic structure. Two different types of the domain walls give rise to the opposite signs of the relaxation. Slow domain wall motion at low temperatures also causes the second relaxation time revealed earlier in a magnetic alternating current (AC) response. A general picture of the magnetic dynamics in $\text{Ca}_3\text{Co}_2\text{O}_6$ comprising of the magnetization curve, response to the AC, and step magnetic fields is discussed.

DOI: [10.1103/PhysRevB.83.092404](https://doi.org/10.1103/PhysRevB.83.092404)

PACS number(s): 75.25.-j, 75.10.Pq, 75.50.Ee

An isolated Ising chain demonstrates specific stochastic magnetization dynamics that originate from an interaction of the chain with an external thermal reservoir.^{1,2} While Ising chains are packed into a non-bipartite two-dimensional (2D) lattice a weak antiferromagnetic (AFM) interchain interaction causes, in addition, a frustration effect. The low dimensionality and frustration lead to a complex magnetic behavior in the spin-chain systems. Presently, few groups of compounds are known in which Ising chains form the frustrated triangular lattice: (i) CsCoCl_3 and CsCoBr_3 ,³ (ii) $\text{Ca}_3\text{Co}_2\text{O}_6$ and related systems,^{4,5} and (iii) $\text{Sr}_5\text{Rh}_4\text{O}_{12}$ discovered recently.^{6,7} A high-temperature phase in all these compounds is unique, namely, it is the partially disordered antiferromagnetic (PDAFM) order or the honeycomb magnetic structure. At low temperatures these systems demonstrate various behavior which appears from weak interactions between next-to-nearest chains.^{7,8} During the last decade most experimental and theoretical efforts on spin-chain compounds were focused on $\text{Ca}_3\text{Co}_2\text{O}_6$ due to its unique magnetic features.^{4,5,8-17}

A crystal structure of $\text{Ca}_3\text{Co}_2\text{O}_6$ consists of Co_2O_6 chains running along the c axis. The Ca ions are situated between them and are not involved in magnetic interactions. The chains are made up of alternating face-sharing CoO_6 trigonal prisms and CoO_6 octahedra. The crystalline electric field causes the high-spin ($S = 2$) ground state of the Co^{3+} ions in the trigonal positions (Co I) and the low-spin ($S = 0$) one in the octahedral environment (Co II). The chains form a triangular lattice in the ab plane that is perpendicular to the chains. It should be mentioned that the topology of the magnetic net in $\text{Ca}_3\text{Co}_2\text{O}_6$ is rather complex since relative shifts of the chains along the c axis give rise to helical paths.¹⁶ An in-chain exchange interaction between high-spin cobalt ions through the octahedra with low-spin cobalt ions is ferromagnetic (FM). The parameter of the FM in-chain coupling (J_1) was determined from the magnetic susceptibility at high temperatures,⁵ specific heat,¹² and theoretical calculations.¹⁶ These estimations are in a reasonable agreement with each other ($J_1 \approx 25$ K). The weak AFM interchain interaction causes the 2D PDAFM structure below $T_1 = 24$ K. At $T_2 \approx 12$ K another magnetic transition takes place^{12,15} that separates the high- and low-temperature phases.

An unusual step-like magnetization curve was found in $\text{Ca}_3\text{Co}_2\text{O}_6$ and widely discussed.^{5,8-16} The number of steps

depends on a sweep rate of the external magnetic field and temperature.^{9,11,13} Two steps become apparent in the temperature range from 12 to 24 K.¹³ At least four equidistant steps are clearly visible below 12 K at a moderate magnetic field sweep rate.^{9,11} At an extremely low-sweep rate the magnetization curve becomes close to the two-step shape, similar to that observed at high temperatures.¹¹

A response to alternating magnetic fields, magnetization relaxation, and their temperature dependence were investigated carefully in Ref. 10. The experimental results show that there exist two characteristic time scales of the magnetization dynamics at low temperatures.

The shape and temperature dependence of the magnetization curve in $\text{Ca}_3\text{Co}_2\text{O}_6$ was qualitatively explained in the framework of the rigid-chain model proposed in Ref. 14. It is based on two main assumptions. (i) The chains are in two ordered states (spin-up or spin-down) at low temperatures. This reduces the problem to the 2D AFM Ising model on the triangular lattice with an AFM nearest-neighbor interaction.¹⁸ (ii) The system is out of equilibrium, that is, it is in a metastable state rather than in the ground one even at a very low-magnetic field sweep rate.¹⁴ The strong dependence of magnetization curve on the magnetic field sweep rate and large hysteresis loop favor this point.^{9,11} At higher temperatures an in-chain disorder is significant and the rigid chain model is no longer valid. In this case, the phase diagram can be discussed in terms of a mean-field model.⁸

To investigate dynamic properties of the spin-chain system the rigid-chain model was supplemented by a single-chain flip rate in the Glauber form,^{17,19} that is, the chains were assumed to interact with a heat reservoir in addition to the nearest-neighbor interaction. Numerical 2D simulation magnetization dynamics has revealed the origin of the second characteristic time scale:¹⁷ a domain structure appears with the magnetic field increase due to the fact that the ferrimagnetic structure on the triangular lattice is threefold degenerate.¹⁷ Slow creep of the domain wall gives rise to a very slow relaxation process. A recent 3D simulation of the Glauber dynamics in $\text{Ca}_3\text{Co}_2\text{O}_6$ has led to the same conclusion.²⁰

The equilibrium magnetization curve was studied by means of the Monte Carlo technique.^{21,22} It was shown that the conventional Metropolis algorithm fails to correctly relax a trial state into the equilibrium state on the AFM triangular

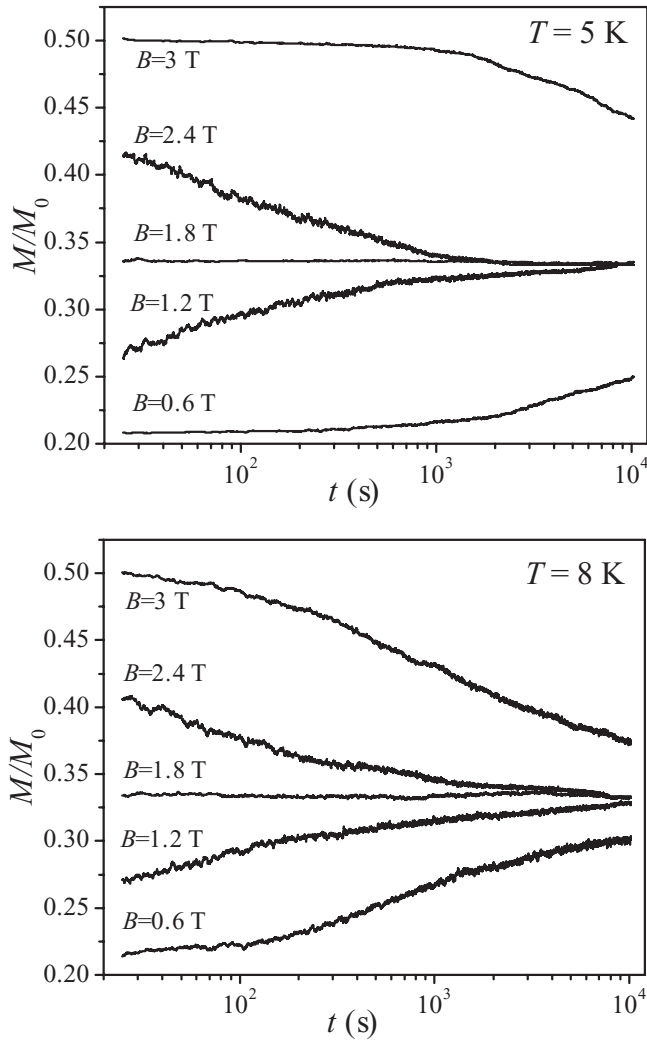


FIG. 1. The response to the step magnetic field (the 2D Glauber model) at different temperatures (the left and right panels) and heights of the step (shown in the figures).

Ising model and the Wang-Landau algorithm (WLA) should be applied instead.²² The WLA gave a two-step magnetization curve on the perfect triangular lattice. In contrast to the Metropolis algorithm, the disorder in a form of a random-exchange term did not change the two-step shape of the magnetization curve. A substitution disorder gave multiple magnetization steps but they were quite different from the four-step curve.²³ These results have led authors of Ref. 22 to the conclusion that the two additional steps in $\text{Ca}_3\text{Co}_2\text{O}_6$ magnetization curve arise from nonequilibrium magnetization dynamics in agreement with the Glauber dynamics.

The purpose of the present paper is an investigation of an unusual response of $\text{Ca}_3\text{Co}_2\text{O}_6$ on a step magnetic field observed in Ref. 11. The following relaxation is very slow and nonexponential. In addition, the sign of the relaxation changes with the step height. If it is below $B = 2.0$ T the magnetization increases during the relaxation, and for the fields above $B = 2.3$ T the magnetization becomes decaying.

The 2D simulation of the response to the step magnetic field was performed on the rhombic 96×96 supercell with the

periodic boundary condition and the same model parameters as we had used previously.¹⁷ An initial randomized state was relaxed at the zero magnetic field. After that the steady magnetic field was switched on. Different simulation runs starting with different random states coincide within the noise. The time dependence of the magnetization at different values of the magnetic field and temperature is shown in Fig. 1. One can see the increasing and decaying branches of the magnetization relaxation. To illustrate their nature we present evolution of the magnetic structure at $B = 1.2$ T and $B = 2.4$ T in Fig. 2. The patterns, which appear just after the field switching on [Figs. 2(a) and 2(c)], are filled with small domains. During the relaxation the patterns rarefies and a characteristic domain size increases [Figs. 2(b) and 2(d)]. Assuming the scaling hypothesis is valid, the divergence of the magnetization Δm from the value corresponding to the monodomain ferrimagnetic structure ($m = \frac{1}{3}$) can be estimated at large time as $\Delta m \propto L \propto a^{-1}$ where L is the boundary length per unit area and a is the characteristic domain size. Thus, it is possible to plot the correlation length [$\propto (\Delta m)^{-1}$] versus the characteristic time and discuss the problem as a dynamic critical phenomenon.²⁴

As it has been established earlier¹⁷ there are two types of the domain boundaries. At the low-magnetic field there appear boundaries with the magnetization deficiency [Figs. 2(a) and 2(b)]. While the magnetic field exceeds $B \simeq 2.2$ T the boundaries transform to other type with the excess magnetization as one can see in Figs. 2(c) and 2(d). This leads to the change of the sign of relaxation which has been observed in the experimental data of Ref. 11. There is a region in the vicinity $B = 2$ T where the domain boundaries of both types coexist [see Fig. 1(c) of Ref. 17]. The two relaxation processes with the opposite signs lead to an almost constant magnetization.

All the results presented above correspond to the field-increasing branch, that is, the magnetic field switches from the zero field to the constant value B . In Ref. 11 the field-decreasing branch, that is a step from a high-magnetic field above the saturation down to B , was also studied. In Fig. 3 the field-increasing and field-decreasing branches obtained by the 2D simulation are compared. There is sizable difference between the relaxation curve depending on the branch. That is, the initial state (zero-field or saturated) strongly affects the domain structure.

An intrachain disorder is beyond the 2D rigid-chain model. To extend the study to the 3D lattice we applied a recent 3D generalization of the Glauber dynamics to $\text{Ca}_3\text{Co}_2\text{O}_6$.²⁰ There is a significant difference in the relaxation between a finite Ising chain and ring (a chain with a periodic boundary condition).^{1,2} That is why a $96 \times 96 \times 36$ supercell with periodic boundary conditions in the ab plane and open chain ends along the c axis was used. The supercell had the real structure of $\text{Ca}_3\text{Co}_2\text{O}_6$ with the shifts of the chains along the c axis. The probability of a spin flip of the i th spin in chain per time unit can be written down in the Glauber form^{17,20}

$$W_i = \frac{\alpha}{2} \left[1 - \sigma_i \tanh \left(\frac{J_1}{kT} \sum_{\langle il \rangle} \sigma_l + \frac{J_2}{kT} \sum_{\langle\langle ij \rangle\rangle} \sigma_j + \frac{\mu B}{kT} \right) \right], \quad (1)$$

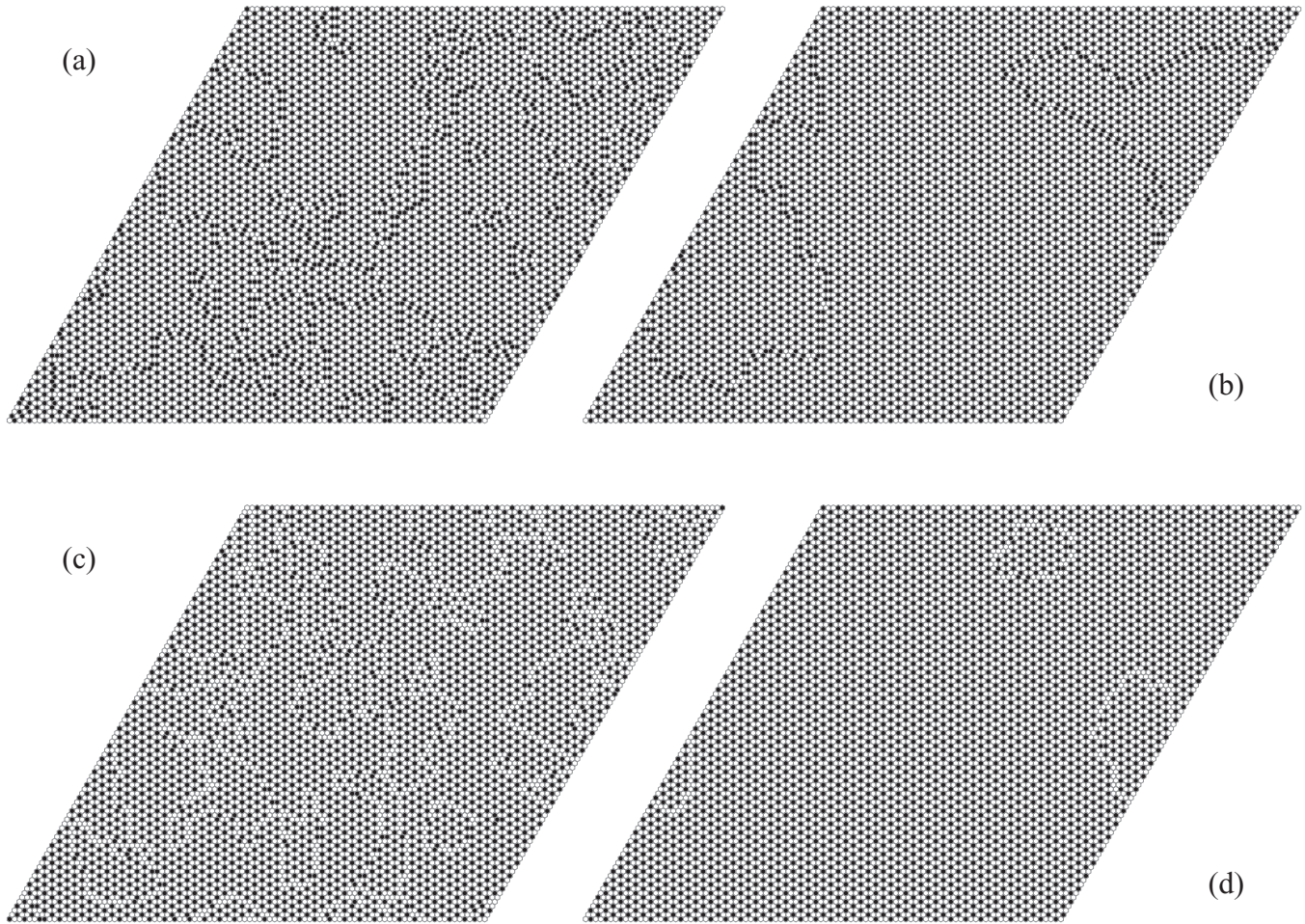


FIG. 2. The relaxation of the magnetization at $B = 1.2$ T (a,b) and $B = 2.4$ T (c,d). The patterns were captured at $t = 125$ s (a,c) and $t = 1250$ s (b,d).

where α is the constant of the interaction of a spin with the heat reservoir, $\sigma = \pm 1$, and $J_1 = 20$ K and $J_2 = -1.6$ K are the parameters of in-chain and interchain interactions,

respectively. k is the Boltzmann constant, T is the temperature, μ is the magnetic moment of the cobalt ion in the high-spin state, B is the applied magnetic field. $\langle \dots \rangle$ and $\langle\langle \dots \rangle\rangle$ denote

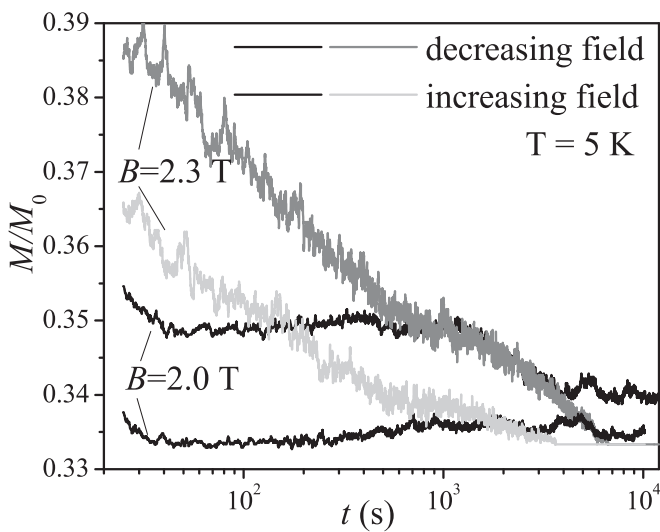


FIG. 3. The field-increasing and field-decreasing branches of the 2D relaxation.

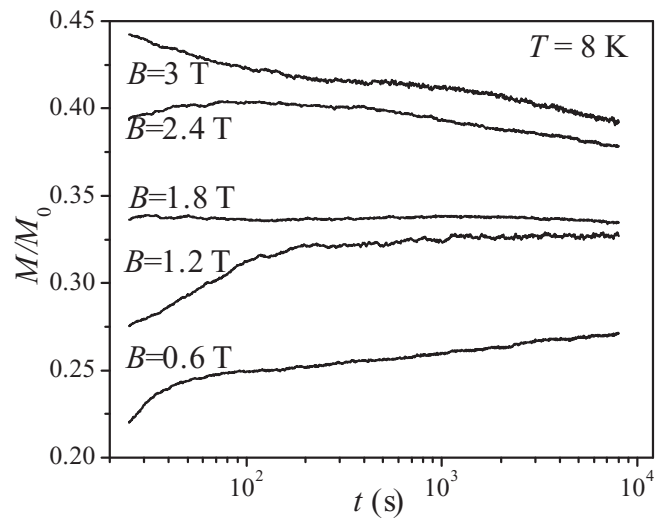


FIG. 4. The magnetization relaxation within the 3D Glauber dynamics.

pairs of the nearest neighbors along the c axis and in the ab plane, correspondingly. The interchain interaction constant was determined from the plateau length in the magnetization curve ($\Delta B = 1.2$ T for $\text{Ca}_3\text{Co}_2\text{O}_6$). Since we do not consider a specific mechanism of the interaction between the reservoir and the chains, α is a free parameter of the model ($\alpha = 20$ s $^{-1}$ for the 3D model). It should be mentioned that the probability of a chain flip in the 2D model has the same form¹⁷ if assumed $J_1 = 0$, $J_2 = -20$ K, and $\alpha = 0.2$ s $^{-1}$. It should be pointed out that the 2D and 3D calculations in Refs. 17 and 20 and the present paper were performed with the same set of parameters.

The 3D simulation takes a large computational burden especially at low temperatures because it should cover two different time scales. The first one corresponds to a flip of a single chain and the second to the slow creep of the domain wall. That is why the number of time points was chosen at least 2×10^7 per pass. The results of the simulation are shown in Fig. 4. General trends of these curves are the same as in Fig. 1, but new features have also appeared. In particular, the curve $B = 2.4$ T demonstrates a nonmonotonic relaxation which was observed experimentally at the same magnetic field.¹¹ The curve lies in the region where both types of the domain boundaries coexist and different relaxation rates form the nonmonotonic shape of the curve.

Within the 3D model a new ingredient to magnetic ordering comes into play, namely the characteristic length of the chains. We have compared results of the 3D simulation on $24 \times 24 \times N$ supercells where $N = 18, 36, 72$ ($T = 8$ K). The relaxation time demonstrated a very weak dependence on the chain length N .

In conclusion, the results obtained complete a general picture of the magnetic dynamics in $\text{Ca}_3\text{Co}_2\text{O}_6$. A frustrated spin-chain system has a complex hierarchy of time scales. The Glauber dynamics reveals two intrinsic times even for a single spin chain.² A characteristic time of about 1 s at $T = 5$ K attributed to the chain flip was found in a previous 2D simulation of the AC response of $\text{Ca}_3\text{Co}_2\text{O}_6$.²⁵ The domain structure arising from the degeneracy of the ferrimagnetic structure on the triangular lattice brings a new time scale of about 10^3 – 10^4 s which was investigated in the present work. Both the characteristic times were observed experimentally in the AC response.¹⁰ A visualization of some of the results can be found in Ref. 26.

The work was supported by Russian Foundation for Basic Research and Russian Federal Education Agency. D.A.M. acknowledges support of the “Dynasty” foundation.

*yu_kudasov@yahoo.com

¹R. Glauber, *J. Math. Phys.* **2**, 294 (1963).

²Y. B. Kudasov, *JETP* **137**, 406 (2010).

³M. Mekata, *J. Phys. Soc. Jpn.* **42**, 76 (1977).

⁴S. Aasland, H. Fjellvåg, and B. Hauback, *Solid State Commun.* **101**, 187 (1997).

⁵H. Kageyama, K. Yoshimura, K. Kosuge, H. Mitamura, and T. Goto, *J. Phys. Soc. Jpn.* **66**, 3996 (1997).

⁶G. Cao, V. Durairaj, S. Chikara, S. Parkin, and P. Schlottmann, *Phys. Rev. B* **75**, 134402 (2007).

⁷Y. B. Kudasov, *JETP Lett.* **88**, 586 (2008).

⁸Y. B. Kudasov, *Europhys. Lett.* **78**, 57005 (2007).

⁹A. Maignan, V. Hardy, S. Hébert, M. Drillon, M. R. Lees, O. Petrenko, D. M. K. Paul, and D. Khomskii, *J. Mater. Chem.* **14**, 1231 (2004).

¹⁰V. Hardy, D. Flahaut, M. R. Lees, and O. A. Petrenko, *Phys. Rev. B* **70**, 214439 (2004).

¹¹V. Hardy, M. R. Lees, O. A. Petrenko, D. McK. Paul, D. Flahaut, S. Hébert, and A. Maignan, *Phys. Rev. B* **70**, 64424 (2004).

¹²V. Hardy, S. Lambert, M. R. Lees, and D. McK. Paul, *Phys. Rev. B* **68**, 14424 (2003).

¹³A. Maignan, C. Michel, A. C. Masset, C. Martin, and B. Raveau, *Eur. Phys. J. B* **15**, 657 (2000).

¹⁴Y. B. Kudasov, *Phys. Rev. Lett.* **96**, 27212 (2006).

¹⁵O. A. Petrenko, J. Wooldridge, M. R. Lees, P. Manuel, and V. Hardy, *Eur. Phys. J. B* **47**, 79 (2005).

¹⁶R. Fresard, C. Laschinger, T. Kopp, and V. Eyert, *Phys. Rev. B* **69**, 140405 (2004).

¹⁷Y. B. Kudasov, A. S. Korshunov, V. N. Pavlov, and D. A. Maslov, *Phys. Rev. B* **78**, 132407 (2008).

¹⁸G. H. Wannier, *Phys. Rev.* **79**, 357 (1950).

¹⁹X. Yao, *Phys. Lett. A* **374**, 886 (2010).

²⁰Y. B. Kudasov, A. S. Korshunov, V. N. Pavlov, and D. A. Maslov, *J. Low Temp. Phys.* **159**, 76 (2010).

²¹X. Y. Yao, S. Dong, and J.-M. Liu, *Phys. Rev. B* **73**, 212415 (2006).

²²M. H. Qin, K. F. Wang, and J. M. Liu, *Phys. Rev. B* **79**, 172405 (2009).

²³X. Yao, *Solid State Commun.* **150**, 160 (2010).

²⁴P. C. Hohenberg and B. I. Halperin, *Rev. Mod. Phys.* **49**, 435 (1977).

²⁵Y. B. Kudasov, A. S. Korshunov, V. N. Pavlov, and D. A. Maslov, *Bull. Rus. Acad. Sci. Phys.* **74**, 6 (2010).

²⁶[http://sarfti.ru/HMFLab/ssph_eng.html].